Self-assembled coumarin- and 5-fluorouracil-PEG micelles as multifunctional drug delivery systems

Sonia López[a], Julián Rodríguez-López[b], M. Teresa García[a], Juan F. Rodríguez[a], José M. Pérez-Ortiz[c], María J. Ramos [a,]*, Ignacio Gracia[a,]*

[a] *Universidad de Castilla- La Mancha, Instituto de Tecnología Química y Medioambiental (ITQUIMA), Departamento de Ingeniería Química, Avda. Camilo José Cela 1A, 13071 Ciudad Real, Spain.*
[b] *Universidad de Castilla-La Mancha, Facultad de Ciencias y Tecnologías Químicas, Área de Química Orgánica, Avda. Camilo José Cela 10, 13071 Ciudad Real, Spain.*
[c] *Hospital General Universitario de Ciudad Real, Unidad de Investigación Traslacional, C/ Obispo Rafael Torija s/n, 13005 Ciudad Real, Spain.*

***Corresponding authors:** mariajesus.ramos@uclm.es (M.J. Ramos); ignacio.gracia@uclm.es (I. Gracia)

Abstract. The copper(I)-catalyzed azide/alkyne cycloaddition is recognized as one of the most successful click reactions to access self-assembling amphiphilic polymer-drug conjugates (PDCs). In this way, poor water-soluble drugs can be linked covalently to hydrophilic poly(ethylene glycol) (PEG) to obtain PEGylated drug micelles that can be used as versatile carriers for the delivery of diverse therapeutic agents. In this work, two novel amphiphilic PDCs that combine PEG with privileged scaffolds well-known for their anticancer properties, such as coumarin and 5-fluorouracil, have been synthesized and characterized. These conjugates were able to self-assemble into micelles at relatively high critical micellar concentration, probably due to the large portion of hydrophilic PEG. The micelles allowed to load other anticancer drugs (paclitaxel, curcumin, and gemcitabine), providing a unique opportunity to develop promising co-delivery carriers for synergistic cancer therapy. The Korsmeyer-Peppas mathematical model was used for describing the *in vitro* kinetics of drug release from the micelles. Similar sustained and controlled drug release profiles were obtained for paclitaxel and curcumin in both conjugates, which was attributed to the excellent stability driven by the strong interaction between polymeric conjugates and drugs in the micelle core. In contrast, the high instability observed for the gemcitabine-loaded micelles provided an initial uncontrolled burst release of drug. A preliminary *in vitro* cytotoxicity study of the micelles against human pancreatic cancer cells PANC-1 and BxPC-3 was also carried out, demonstrating that both coumarin and 5-fluorouracil retain their anticancer properties after conjugation with PEG.

Keywords: anticancer, polymer-drug conjugates, drug delivery, micelles, click chemistry.

Highlights

- Two novel amphiphilic polymer-drug conjugates (PDCs) were prepared via CuAAC reaction.

- These PDCs combine PEG with anticancer agents, such as coumarin and 5-fluorouracil.

- They can self-assemble into micelles and encapsulate other anticancer drugs.

- The micelles exhibit antiproliferative activity against PANC-1 and BxPC-3 cells.

- Promising co-delivery carriers for synergistic cancer therapy can be developed.

1. Introduction

Cancer is among the leading causes of death worldwide. Millions of people around the world are diagnosed with cancer annually, and more than half of patients eventually die from it [1,2]. Moreover, based on current trends, cancer cases are expected to increase as a result of population ageing and the adoption of unhealthy lifestyles and habits [3].

Numerous and innovative drugs have been developed to treat cancers. Nevertheless, the therapeutic effect of conventional treatments is typically compromised by low bioavailability and specificity, generating severe systemic toxicity. Tremendous efforts have been made to overcome these and other issues and improve the therapeutic benefit of cancer therapies [4].

Recently, nanocarriers have generated a growing interest due to the numerous aspects that remarkably influence the efficacy of treatments [5]. They can be formulated with several materials, e.g., liposomes, polymers (macromolecules, micelles o dendrimers) and viruses (viral-like nanoparticles) [6,7]. Among them, polymeric micelles have emerged as promising nanoparticles for the delivery of poorly soluble anticancer agents. Micelles are formed by the self-assembly of amphiphilic polymers to give nano-sized vesicles with relatively high stability [8]. These characteristics prolong the blood half-life of chemotherapeutic agents that can passively accumulate in tumors, especially in poorly vascularized tumors. The hydrophobic drug can be physically encapsulated in the micelle [9] or linked covalently to the polymer to give a self-assembling amphiphilic polymer-drug conjugate (PDC) [10,11]. Poly(ethylene glycol) (PEG) is the most widely used hydrophilic polymer because it acts as an efficient steric protector, shows a high degree of biocompatibility, has low toxicity, and has been approved by the Food Drug Administration (FDA) [12]. Thus, poor water-soluble drugs can be conjugated with PEG to obtain PEGylated drug micelles [13].

Many creative conjugation strategies have been proposed to furnish PDCs with functions that make them competent in specific applications, including pharmaceutical. In this context, the click chemistry has emerged as a powerful and chemoselective tool for the attachment of targeting ligands to polymeric drug carriers [14]. In particular, the copper(I)-catalyzed azide/alkyne cycloaddition (CuAAC) has shown as one of the most prolific and successful click reactions, characterized by high yields and selectivity with little or no by-products [15,16]. The regioselective 1,2,3-triazole ring formed in this reaction is a favorable linker that displays a marked stability to hydrolytic, oxidizing, and reducing conditions. It also resists metabolic degradation and can favor the binding of biomolecular targets, substantially enhancing the pharmacological activity [17]. Thus, it is a very well-recognized pharmacophore that has been widely exploited in the development of anticancer agents [18].

In this work, 4-azidomethyl-7-methoxycoumarin (AMMC) and 1,3-bis(5-azidopentyl)-5-fluorouracil (5-FUDA) were conjugated to methoxy PEG alkyne (mPEG-alkyne, molecular weight 2000 Da) via click chemistry to prepare two amphiphilic PDCs, **CouPEG** and **5-FUPEG**, respectively. Both coumarin and 5-fluorouracil are privileged scaffolds well-known for their anticancer properties [19,20]. The novel amphiphilic conjugates self-assembled into micelles that were used to encapsulate other anticancer drugs such as paclitaxel (PTX), curcumin (CUR), and gemcitabine (GEM), providing a unique opportunity to exploit the potential synergy of dual/multiple therapy (Figure 1). Paclitaxel is highly lipophilic and has a powerful anticancer effect on pancreatic, ovarian, breast, and non-small cell lung

cancers [21]. Curcumin possesses various beneficial activities for human health, such as antioxidant, antiviral, anti-inflammatory, and anticancer agent (included pancreatic cancer) [22,23]. Nevertheless, its effectiveness is limited due to low water solubility, poor oral bioavailability, and rapid systemic elimination. Gemcitabine is a potent hydrophilic drug approved for the treatment of an unusually broad spectrum of tumors, although it shows a severely limited therapeutic efficacy due to its rapid metabolic inactivation [24]. Due to the pharmacological strength and limitations of these drugs, they were chosen as a model to explore the drug loading capacities and release profiles of the **CouPEG** and **5-FUPEG** micelles. The drug release data were fitted to the Korsmeyer-Peppas model to predict the kinetics and release mechanisms. Finally, a preliminary *in vitro* cytotoxicity assay of the blank micelles against human pancreatic cancer cell lines PANC-1 and BxPC-3 was carried out.

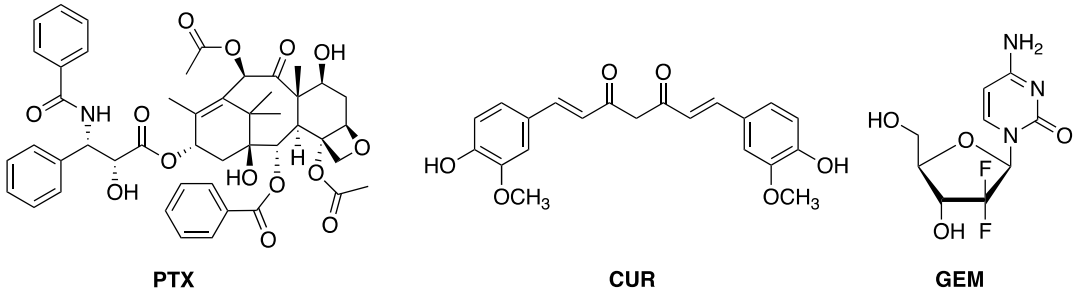

Figure 1. Chemical structures of paclitaxel (PTX), curcumin (CUR), and gemcitabine (GEM).

2. Experimental

2.1. Materials and methods

5-Fluorouracil, curcumin, gemcitabine hydrochloride, methoxy poly(ethylene glycol) alkyne (mPEG-alkyne, 2000 g/mol), copper wire (diameter 0.25 mm), and carbon dioxide (purity 99.8%) were obtained from commercial sources and used without further purification. Paclitaxel was provided by the Hospital General de Ciudad Real (Spain). 1-Azido-5-bromopentane (ABrP) was prepared according to a literature procedure [25,26]. 4-Azidomethyl-7-methoxycoumarin (AMMC) was prepared as described elsewhere by some of us [27]. All other chemicals used for this study were provided by domestic suppliers and were analytical grade.

NMR spectra were acquired at room temperature on a Bruker Advance Neo 500 or a Bruker Advance Neo 400 spectrometer. The chemical shifts (δ) are reported in ppm and are referenced internally to the solvent signals of $CDCl_3$ (^1H, δ = 7.27 ppm; ^{13}C, δ = 77.0 ppm) or externally to $CFCl_3$ (^{19}F, 0.0 ppm). The coupling constants *J* are given in Hz. In the ^1H NMR spectra, the following abbreviations are used to describe the peak patterns: s (singlet), d (doublet), t (triplet), m (multiplet). In the ^{13}C NMR spectra, the nature of the carbons (C, CH, CH_2 or CH_3) was determined by performing a DEPT experiment. Gel Permeation Chromatography (GPC) measurements were performed with a Viscotek chromatograph with two columns (Styragel HR2 and Styragel HR0.5) at 35 °C with a flow of 1 mL·min^{-1} and THF as eluent. The IR spectra were recorded with a with a Jasco FT/IR-4700 or a PerkinElmer spectrophotometer equipped with an attenuated total reflectance (ATR) accessory. MALDI-TOF mass spectra were carried out using a Bruker Autoflex II TOF/TOF spectrometer in positive detection mode, using dithranol as matrix. Elemental analyses were performed in a Thermo Scientific Flash Smart elemental analyzer.

2.2. Synthesis of conjugates

2.2.1. Synthesis of 1,3-bis(5-azidopentyl)-5-fluorouracil (5-FUDA).

A solution of 5-fluorouracil (260 mg, 2 mmol), 1-azido-5-bromopentane (802 mg, 4.2 mmol), and 1,8-diazabicyclo[5.4.0]undec-7-ene (DBU, 850 µL, 6 mmol) in acetonitrile (5 mL) was heated under reflux for 1.5 h under argon. After cooling, 1M aqueous HCl was added and the mixture was extracted with EtAcO (×3). The combined organic layers were dried ($MgSO_4$), the solution filtered, and the solvent evaporated under reduced pressure. The crude product was purified by column chromatography (silica gel, hexanes/EtAcO, 6:4) to give 388 mg (81%) of the title product as a colorless oil. ^{1}H NMR ($CDCl_3$, 500 MHz) *δ*: ^{1}H NMR ($CDCl_3$, 500 MHz) δ: 7.21 (d, 1H, *J* = 5.5 Hz, CH=), 3.98 (t, 2H, *J* = 7.5 Hz, CH_2), 3.74 (t, 2H, *J* = 7.5 Hz, CH_2), 3.33-3.26 (m, 4H, 2×CH_2), 1.78-1.62 (m, 8H, 4×CH_2), 1.47-1.40 (m, 4H, 2×CH_2). ^{13}C NMR and DEPT ($CDCl_3$, 125 MHz) *δ*: 157.1 (d, *J* = 24.7 Hz, CF-CO-NH), 149.8 (NH-CO-NH), 140.0 (d, *J* = 233.9 Hz, C-F), 126.3 (d, *J* = 32.0 Hz, CH=), 51.2 (CH_2), 51.0 (CH_2), 49.7 (CH_2), 41.7 (CH_2), 28.4 (CH_2), 28.4 (CH_2), 26.9 (CH_2), 23.9 (CH_2), 23.6 (CH_2). ^{19}F NMR ($CDCl_3$, 470 MHz) δ: –164.4. IR (ATR) *ν*: 2089 (N_3), 1712, 1680, 1649, 1469, 1349, 1257, 758 cm^{-1}. MALDI-TOF MS (dithranol) *m/z*: 325.3 [M+H–N_2]$^+$. Anal. Calcd for $C_{14}H_{21}FN_8O_2$: C, 47.72; H, 6.01; N, 31.80. Found: C, 47.75; H, 6.03, N, 31.88.

*2.2.2. Synthesis of mPEG-coumarin (**CouPEG**).*

The synthesis of CouPEG was performed in supercritical CO_2 ($scCO_2$) according to a previous work [25].¡**Error! Marcador no definido.** Equimolar amounts of mPEG-alkyne (11.6 mg, 0.05 mmol) and AMMC (105 mg, 0.05 mmol) together with copper wire (317 mg, 5 mmol) were reacted at 13 MPa and 35 ºC for 24 h. After cooling, the reactor was depressurized with a flow rate of 3 L/min and tweezers were used to separate the copper. The title compound was obtained as a yellow solid (101 mg, 96%). The characterization spectra can be found in the Supplementary Material.

*2.2.3. Synthesis of mPEG-5-fluorouracil (**5-FUPEG**).*

A mixture of mPEG-alkyne (400 mg, 0.2 mmol), 5-FUDA (35 mg, 0.1 mmol), *N,N,N′,N″,N″*-pentamethyldiethylenetriamine (PMDTA, 17 mg, 0.1 mmol), copper wire (635 mg, 10 mmol), and PMDTA (17 mg, 0.1 mmol) in dry toluene (10 mL) was heated to 80 ºC and stirred for 48 h under argon atmosphere. Then, the copper was removed and the solvent evaporated under vacuum. The crude product was dissolved in a small amount of CH_2Cl_2, filtered through a short pad of celite®, concentrated to dryness, and washed with ether. After dissolving in Milli-Q water, purification from excess mPEG-alkyne was performed by passing through an Amicon® Ultra-4 Centrifugal Filter 3K device. The title compound was obtained by lyophilization as a white solid (190 mg, 81%). The characterization spectra can be found in the Supplementary Material.

2.2.4. Molecular weight distribution.

The molecular weight and molecular weight distribution of conjugates was determined by MALDI-TOF mass spectrometry and GPC. The number average (M_n) and weight average (M_w) molecular weights were calculated according to Equations 1 and 2. Additionally, the polydispersity index (PDI) was obtained as a function of the molecular weights (Equation 3) [28].

$$M_n = \sum(N_i \cdot M_i) / \sum N_i \quad (1)$$

$$M_w = \sum(N_i \cdot M_i^2) / \sum(N_i \cdot M_i) \quad (2)$$

$$PDI = M_w/M_n \quad (3)$$

where M_i is the molecular weight of a chain and N_i the corresponding signal intensity.

2.3. Determination of critical micellar concentration (CMC).

The critical micellar concentration (CMC) of conjugates was determined by using the iodine UV-vis spectroscopy method following a reported procedure [29]. **CouPEG** and **5-FUPEG** concentrations ranging from 0.0001 mg/mL to 0.7 mg/mL were prepared with Milli-Q water as solvent. Measurements were performed at 366 nm. Each experiment was repeated three times and the average absorbance was determined.

2.4. Preparation and characterization of drug-loaded polymeric micelles.

*2.4.1. Preparation of **CouPEG** and **5-FUPEG** micelles loaded with PTX, CUR, and GEM.*

PTX-, CUR- and GEM-loaded micelles were prepared by an organic solvent evaporation method at different drug/polymer ratios of 1:10, 2:10, and 3:10 wt/wt. Thus, 100 mg of the corresponding polymeric conjugate (**CouPEG** and **5-FUPEG**) was dissolved in 10 mL Milli-Q water and a solution of drug in $CHCl_3$ (PTX, CUR, GEM) was added dropwise under gentle stirring for 4 h. Then, the emulsion was sonicated and the organic solvent removed under vacuum using a rotary evaporator (Figure S1, Supplementary Material). Finally, the micellar solution and the unentrapped drug were separated by centrifugation at 3800 rpm (3150 xg) for 4 h. The supernatant with the drug loaded into the core of the micelles was isolated to further characterization and the unentrapped drug was analyzed to determine the encapsulation efficiency (EE).

2.4.2. Encapsulation efficiency and drug loading

The amount of PTX, CUR, and GEM encapsulated into the micelles was determined by UV-vis spectroscopy. After centrifugation, the free drug was dried overnight at 40 °C to avoid degradation. Then, 1 mL of the appropriate solvent was added, the mixture sonicated for 2-3 minutes, and the absorbance measured at 230, 425, and 268 nm for PTX, CUR, and GEM, respectively. The calibration curves of each drug are included in the Supplementary Material (Figures S2-S4). The encapsulation efficiencies and drug loading were calculated using the Equations 4 and 5, respectively.

$$\text{Encapsulation efficiency (\%)} = \frac{\text{Total amount of drug} - \text{Amount of free drug}}{\text{Total amount of drug}} \cdot 100 \quad (4)$$

$$\text{Drug loading (\%)} = \frac{\text{Total amount of drug} - \text{Amount of free drug}}{\text{Amount of conjugated used}} \cdot 100 \quad (5)$$

2.4.3. Particle morphology

Micellar morphology was studied by scanning electron microscopy (SEM) using a Quanta 250 equipment with a wolfram filament operating at a working potential of 10 kV (FEI Company). Samples were prepared by dropwise addition of the solution onto the pin, followed by evaporation of the solvent in air.

2.4.4. Determination of size and zeta potential

The average diameter, size distribution, and zeta potential (ζ) of micelles were measured by dynamic light scattering (DLS) on a Zetasizer Nano ZSP of Malvern. The light source was a 10 mW He-Ne laser operating at a fixed wavelength of 633 nm, scattering angle of 90°, and 37.5 °C of temperature (the corporal temperature, approximately). The stability of micelles was analyzed by ζ measurements, using the laser Doppler microelectrophoresis technique with fitting to Smoluchowski equation. This procedure allows to determine ζ of particle suspensions with a diameter comprised within 3.8 nm to 100 µm. All the measurements were done in triplicate.

2.4.5. In vitro drug release profiles.

The *in vitro* drug release study was conducted by placing a dialysis bag (molecular weight cut off, MWCO: 3500 g/mol) containing 10 mL of drug-loaded micelles solutions (0.5 mg/mL) into 90 mL of a stirred phosphate buffer solution (PBS, pH 7.4 physiological) at 37.5 ºC. The bag was closed on both sides with clips. Periodically, aliquots of 10 mL were withdrawn and refilled with 10 mL fresh PBS. The collected samples were lyophilized and then dissolved in 4 mL of the adequate solvent. The calibration curves described in section 2.4.2 (Figures S2-S4) were used to determine the amount of drug released (Equation 6). The cumulative drug release (CDR) was calculated using the Equation 7.

$$\text{Amount of drug released (mg/mL)} = \frac{\text{Concentration} \cdot \text{Dissolution bath volume} \cdot \text{dilution factor}}{1000} \quad (6)$$

$$\text{Cumulative percentage of release (\%)} = \frac{\text{Amount of drug released}}{\text{Total amount of drug loaded}} \cdot 100 \quad (7)$$

2.4.6. Drug release kinetics

The most widely used mathematical model to analyze and describe the mechanism by which the release process occurs was developed by Korsmeyer and Peppas [30-31]. After plotting the release profile curves (cumulative percentage of release against time), this mathematical model was applied to determine the kinetics of drug release from the micelles (Equation 8). The Excel software was used to fit the release curve.

$$M_t/M_\infty = k \cdot t^n \quad (8)$$

M_t is the amount of drug released at time t, M_∞ is the total amount of drug released at infinite time, k is the rate of drug release from the polymeric micelles (the release rate constant) which depends on the structural and geometrical characteristic of the particles; t is the release time; and n is the diffusional exponent which indicates the drug release mechanism. According to Ritger and Peppas [32], when n = 0.43 the release mechanism follows a Fickian diffusion. When n = 0.85, a polymer swelling control occurs (case II transport). Otherwise, the mechanism was governed by a combination of diffusion and erosion control ($n < 0.43$) or anomalous transport mechanism ($0.43 < n < 0.85$). The value of $n > 0.85$ is considered a super case II transport.

2.4.7. In vitro MTT assay

An *in vitro* MTT [3-(4,5-dimethylthiazol-2-yl)-2,5-diphenyltetrazolium bromide] assay was used to assess the cytotoxic activity of **CouPEG** and **5-FUPEG** conjugates against PANC-1 and BxPC-3 cells. The MTT assay is based on the conversion of MTT into formazan crystals by living cells, which determines mitochondrial activity. Thus, 10,000 PANC-1 cells per well were seeded in 96-well plates in DMEM (Dulbecco's Modified Eagle's medium, 100 mL). The cells were allowed to adhere to the bottom of the well and incubated overnight at 37 ºC and 5% CO_2. The culture medium was replaced by fresh DMEM containing polymer conjugate at different concentrations: **CouPEG** (25.6 and 51.0 µg/mL) and **5-FUPEG** (14.5, 22.4, 29.0, and 44.8 µg/mL). After 24 and 40 h, the cells were washed with PBS for three times and incubated with medium for 2 h. The cells were incubated for 24 h (37 ºC, 5% CO_2). The absorbance of MTT was measured in a Dynex Spectra MR (Chantilly, VA, USA) at 570 nm with background subtracted at 650 nm. All values were normalized with respect to control wells as indicated in Equation 9. Each experiment was conducted in sextuplicate, and the average data are presented.

$$\text{Cell Viability (\%)} = (\text{Absorbance}_{\text{treated}}/\text{Absorbance}_{\text{control}}) \times 100 \quad (9)$$

3. Results and discussion

3.1. Synthesis and characterization of amphiphilic conjugates CouPEG and 5-FUPEG.

The amphiphilic polymer-drug conjugates were prepared by CuAAC from mPEG-alkyne (MW 2000 g/mol) and the corresponding azide derivatives with Cu wire as catalyst. Supercritical carbon dioxide ($scCO_2$) was used as reaction medium for the synthesis of **CouPEG**. Unfortunately, the supercritical conditions were not very favorable to access **5-FUPEG**. In this case, more classical reaction conditions (toluene, 80 ºC, PMMT as ligand) provided cleaner crude products, which were consequently easier to purify (Scheme 1). Firstly, 1,3-bis(5-azidopentyl)-5-fluorouracil (5-FUDA) was obtained by reaction of 5-fluorouracil (**5-FU**) with 1-azido-5-bromopentane (ABrP) under basic conditions (DBU) (Figures S5-S10).

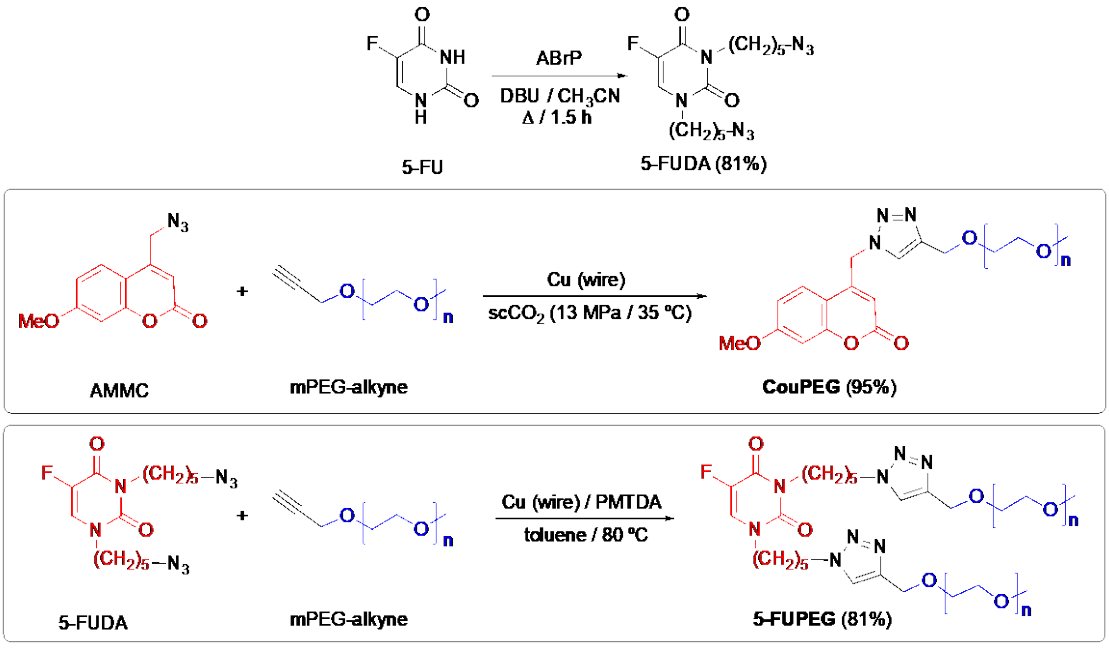

Scheme 1. Synthesis of 5-FUDA, **Cou-PEG**, and **5-FUPEG**.

Both conjugates were satisfactorily characterized by a variety of analytical techniques. While the ^{1}H NMR spectra showed the characteristic triazole protons as singlets at 7.56-7.73 ppm (Figures S11-S12, Supplementary Material), the complete disappearance of the typical azide band at 2084 cm^{-1} and the terminal acetylene band at 2167 cm^{-1} of the starting materials in the IR spectra confirmed the success of the above reactions (Figure S13). The molecular weight and molecular weight distribution (polydispersity) of conjugates was determined by MALDI-TOF mass spectrometry and GPC (Figures S14-S15). Table 1 summarizes the results obtained, which also indicated the successful binding of AMMC (231 g/mol) and 5-FUDA (352 g/mol) to mPEG-alkyne yielding **CouPEG** and **5-FUPEG**, respectively. The values for **CouPEG** were in good agreement with those previously published [27].

Table 1. Molecular weight and polydispersity of conjugates determined by MALDI TOF mass spectrometry and GPC.

	MALDI TOF MS			GPC		
Compound	$\mathbf{M_n}$	$\mathbf{M_w}$	**PDI**	$\mathbf{M_n}$	$\mathbf{M_w}$	**PDI**
mPEG-alkyne	2027.57	2140.27	1.06	1786	1862	1.04
CouPEG	2256.35	2364.34	1.05	1990	2158	1.08
5-FUPEG	4242.00	4048.03	1.00	3885	3987	1.03

3.2. Preparation and characterization of micelles.

It is well known that molecules with suitable hydrophobic and hydrophilic components can form aggregates when exposed to selective solvent. Whereas PEG is well-known for its hydrophilic nature, AMMC and 5-FUDA are hydrophobic small molecules with an octanol-water partition coefficient $logP_{o/w}$ value of 2.45 and 3.04, respectively (estimated using online Molinspiration Cheminformatics software) [33]. In this way, the amphiphilic conjugates **CouPEG** and **5-FUPEG** could self-assemble into regular micelles in aqueous solution, which could be used to load hydrophobic, poorly water-soluble drugs as explained below. The critical micelle concentration (CMC) was determined at 36 ºC using the iodine UV-vis spectroscopy method (see section 2.3). The absorption intensity of I_2 was plotted against the logarithm of the concentration of each conjugate to give a curve where the point of inflection was equal to CMC. We obtained CMC values of 0.09 mg/mL and 0.19 mg/mL for **CouPEG** and **5-FUPEG**, respectively (Figure 2). These relatively high CMC values for both conjugates may be explained by the large portion of hydrophilic PEG. Similar results have also been reported in previous works [34,35]. The presence of two hydrophilic PEG chains in the structure of **5-FUPEG** led to a higher CMC than that of **CouPEG**.

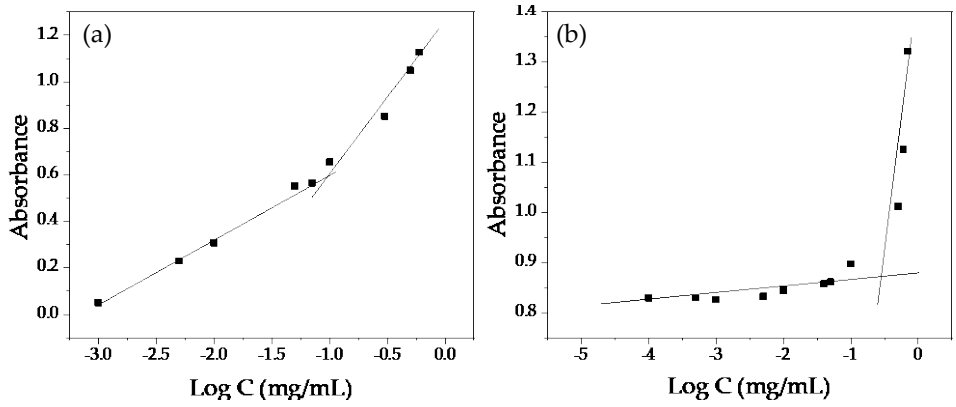

Figure 2. Determination of CMC for (a) **CouPEG** and (b) **5-FUPEG**.

3.3. Preparation and characterization of drug-loaded polymeric micelles

To verify the potential of the **CouPEG** and **5-FUPEG** micelles as delivery systems, three drugs (PTX, CUR and GEM) were physically encapsulated into them at different drug/conjugate (D/C) ratios of 1:10, 2:10, and 3:10 wt/wt. The polymer concentration was fixed in this study at 10 mg/mL. The drug loading (DL) capacity and the encapsulation efficiency (EE) are summarized in Table 2.

Table 2. Drug loading (DL) and encapsulation efficiency (EE) of PTX, CUR, and GEM into **CouPEG** and **5-FUPEG** micelles.

		CouPEG			**5-FUPEG**		
Drug		**D/C 0.1**	**D/C 0.2**	**D/C 0.3**	**D/C 0.1**	**D/C 0.2**	**D/C 0.3**
PTX	DL	13.2 ± 2.5	14.0 ± 2.0	16.7 ± 4.0	6.7 ± 2.0	8.7 ± 3.5	9.4 ± 4.3
	EE	52.3 ± 1.6	88.9 ± 1.7	77.2 ± 1.0	23.1 ± 1.2	45.6 ± 1.6	60.1 ± 5.5
CUR	DL	6.2 ± 2.0	16.9 ± 3.5	24.1 ± 4.3	3.2 ± 2.5	5.7 ± 2.0	8.9 ± 4.0
	EE	45.3 ± 1.6	64.5 ± 1.7	75.4 ± 5.5	18.1 ± 1.6	21.3 ± 1.7	45.7 ± 1.0
GEM	DL	4.0 ± 0.5	6.7 ± 1.0	8.6 ± 1.2	4.8 ± 1.0	5.3 ± 1.0	6.2 ± 1.2
	EE	15.6 ± 2.6	23.4 ± 2.7	24.2 ± 2.0	16.1 ± 0.8	17.5 ± 0.3	15.9 ± 1.3

In general, the **CouPEG** micelles exhibited the highest DL capacity and EE. In all cases, the DL increased as the amount of drug increased. A similar trend was observed for EE, except when the micelles were loaded with PTX. In this case, the percentage of EE decreased by 11.7% (from 88.9% to 77.2%) when the D/C ratio increased from 0.2 to 0.3, which can be explained by the limited solubilization capacity of the micelles [36,37]. These results suggested that **CouPEG** was an excellent carrier for PTX and CUR. The high loading capacity of this system was ascribed to the strong hydrophobic and π-π interactions between the coumarin unit and the aromatic groups of PTX and CUR in the micelle core [38]. A similar increasing trend was found for both parameters in the **5-FUPEG** micelles, although with lower values probably due to the weaker hydrophobicity of **5-FUPEG**. Gemcitabine hydrochloride, with a high-water solubility (> 15 mg/mL at pH = 2.7-9.0), led to the lowest DL and EE values in both **CouPEG** and **5-FUPEG** micelles.

Important parameters for drug delivery systems such as the hydrodynamic particle size and size distribution (polydispersity index, PDI) were evaluated by DLS (Table 3). Both suffered significant changes when the different drugs were loaded into the micelles.

Table 3. Physicochemical characterizations of micelle formulations (mean ± SD, n = 3).[a]

Conjugate	Drug	D/C Ratio	Particle size (nm)	PDI	ξ Potential (mV)
ΩCouPEG	Blank	-	86.10 ± 50.1	0.063	-33.1 ± 0.3
	PTX	0.1	178.3 ± 12.67	0.270	-26.8 ± 0.42
		0.2	299.5 ± 14.68	0.129	-31.83 ± 1.31
		0.3	360.1 ± 19.08	0.057	-31.3 ± 1.32
	CUR	0.1	268.1 ± 22.40	0.163	-30.9 ± 2.50
		0.2	380.4 ± 36.13	0.224	-28.3 ± 0.78
		0.3	390.5 ± 23.63	0.219	-29.5 ± 0.72
	GEM	0.1	201.9 ± 51.56	0.369	-11.6 ±2.02
		0.2	228.0 ± 36.95	0.437	-11.7 ± 3.4
		0.3	328.0 ± 113.3	0.415	-11.3 ± 5.3
5-FUPEG	Blank	-	104.6 ± 38.3	0.180	-31.8 ± 0.13
	PTX	0.1	116.9 ± 70.53	0.267	-24.2 ± 5.46
		0.2	142.1 ± 38.1	0.241	-25.0 ± 3.36
		0.3	382.3 ± 88.1	0.424	-27.5 ± 4.67
	CUR	0.1	132.0 ± 11.6	0.204	-29.2 ± 2.12
		0.2	234.1 ± 23.4	0.353	25.7 ± 1.49
		0.3	381.4 ± 5.3	0.286	26.9 ± 3.69
	GEM	0.1	321.6 ± 42.3	0.423	-4.70 ± 4.65
		0.2	137.8 (60.6%) ± 57.5 469.2 (39.4%) ± 133.4	0.367	-3.97 ± 4.28
		0.3	368.0 ± 126.8	0.560	-3.18 ± 4.28

[a] SD: standard deviation.

The average diameter of the **CouPEG** and **5-FUPEG** micelles was 86.1 ± 50.1 nm and 104.6 ± 38.3 nm, respectively. As expected, the encapsulation of a drug resulted in an increase of micellar size [39]. The higher the D/C ratio, the larger the size of the micelles. Whereas most drug-loaded micelles showed a monodispersed size distribution, GEM-loaded **5-FUPEG** micelles exhibited a bimodal distribution for D/C ratios of 0.2 and 0.3, indicating that the aqueous micellar solutions contained two distinct populations of small and large particles (see DLS histograms in the Supplementary Material, Figure S16). These bimodal distributions were probably a result of a secondary association of micelles [40]. In fact, the small particles occupied the majority in the particle groups. The PDI values obtained for the PTX- and CUR-loaded **CouPEG** micelles, close to or less than 0.2, may be considered acceptable for drug delivery applications and indicated a homogeneous population [41]. Nevertheless, GEM-loaded **CouPEG** and drug-loaded **5-FUPEG** micelles exhibited PDI > 0.3 in most cases, although never greater than 0.7. Values above 0.7 indicate a very broad particle size distribution in the sample. SEM images revealed a spherical morphology in all cases (Figure S17, Supplementary Material).

The zeta potential (ξ) is one of the key parameters to determine the physical stability of the micelles as well as their cell adhesion. An absolute value of ± 30 mV is often used as a stability threshold. In general, higher negative values ensure greater stabilities and reduce occasional aggregation. The zeta-potential measurements showed that micelles, especially **CouPEG** micelles, remained stable after loading with PTX and CUR, with ξ values close to − 30 mV. In contrast, the absolute ξ potential value was < 30 mV when GEM was loaded, giving rise to unstable micelles.

3.4. In vitro drug release and kinetic modeling

The *in vitro* release behavior of PTX, CUR, and GEM from **CouPEG** and **5-FUPEG** micelles was investigated in PBS (pH = 7.4) at 37 ºC for 90 h. The percentage of cumulative drug release (CDR) was plotted against time to obtain the drug release profiles (Figure 3).

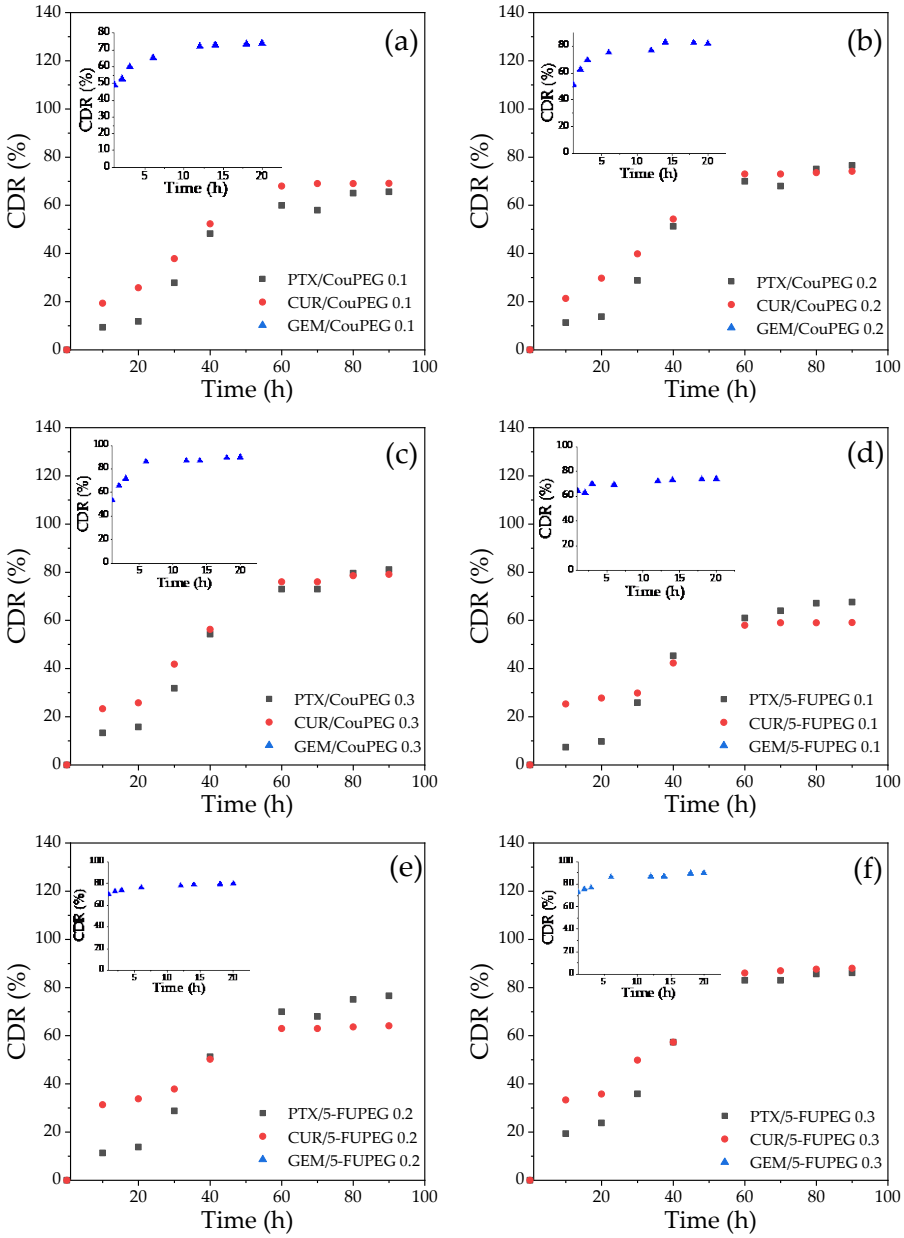

Figure 3. *In vitro* release profiles of PTX, CUR, and GEM from drug-loaded **CouPEG** and **5-FUPEG** micelles in PBS at 37 ºC. (a) Drug/**CouPEG** ratio 0.1; (b) drug/**CouPEG** ratio 0.2; (c) drug/**CouPEG** ratio 0.3; (d) drug/**5-FUPEG** ratio 0.1; (3) drug/**5-FUPEG** ratio 0.2; and (f) drug/**5-FUPEG** ratio 0.3.

Most polymer drug delivery systems exhibit an initial burst release of the drug that takes place in the first few hours. An excessive burst release is normally undesirable because it shortens the overall duration of the therapeutic effect and can cause toxicity [42]. In this study, similar profiles were obtained for PTX and CUR in both conjugates. There is a steady, continued-release pattern of the drug in the first

40 h, after which the percentage of CDR remains nearly constant. The CDR was found to increase slightly with increasing the D/C ratio. Around 20-40% of drugs were retained in the micelles after 90 h [43]. This sustained and controlled release was attributed to the excellent stability driven by the strong interaction between polymeric conjugates and drugs. In contrast, a burst release was initially observed for GEM. The released amount of GEM (0.3 D/C Ratio) for **CouPEG** and **5-FUPEG** at 6 h was 86% and 88%, respectively. In this case, the fast drug release was ascribed to the high instability of the micelles, as discussed in the previous section.

In order to better understand the drug release profiles and predict *in vivo* performance, the Korsmeyer-Peppas model was used to investigate the release of the three drugs studied at 0.3 D/C ratio [30-32]. The fitted theoretical profiles based on the experimental release data, the calculated drug release exponent n, and rate constant k are shown in Table 4 (see also Figure S18).

The releasing profiles were divided into two stages: a rapid release over the first hours (the first 40 h for PTX and CUR; the first 12 h for GEM) followed by a gradual and stable release (up to 90 h for PTX and CUR; 20 h for GEM).

Table 4. Data fitted to the Korsmeyer-Peppas model to describe the *in vitro* release kinetics (mean ± SD).

D/C ratio 0.3	**CouPEG**						**5-FUPEG**					
	n	***k* (h^{-1})**	**R^2**	***n***	***k* (h^{-1})**	**R^2**	***n***	***k* (h^{-1})**	**R^2**	***n***	***k* (h^{-1})**	**R^2**
	0-40 h			**40-90 h**			**0-40 h**			**40-90 h**		
PTX	1.35 ± 0.20	0.002	0.969	0.34 ± 0.07	0.216	0.718	1.02 ± 0.01	0.010	0.996	0.12 ± 0.31	0.579	0.718
CUR	0.86 ± 0.12	0.021	0.922	0.13 ± 0.32	0.550	0.718	0.54 ± 0.06	0.074	0.911	0.07 ± 0.04	0.717	0.989
	0-12 h			**12-20 h**			**0-12 h**			**12-20 h**		
GEM	0.25 ± 0.32	0.782	0.945	0.07 ± 0.45	0.809	0.530	0.08 ± 0.12	0.766	0.872	0.06 ± 0.45	0.833	0.655

For PTX- and CUR-loaded micelles, the *n* values were above 1 in the first stage and well below 0.43 in the second stage. These values indicated that the release behaviors correspond to a super case II mechanism in the first 40 h, where the release is governed by macromolecular relaxation of the polymer chains, and change to a combination of diffusion and erosion control in the second stage. For the GEM-loaded micelles, the release mechanism is controlled by diffusion and erosion in both stages. On the other hand, the *k* values indicated a gradual drug release for PTX and CUR-loaded micelles, although *k* experienced an increase in the second stage after a very slow first stage. In contrast, the *k* values were much higher and almost constant at both stages for GEM-loaded micelles, which resulted in a rapid drug release.

3.5. Preliminary study of in vitro anticancer efficacy of CouPEG and 5-FUPEG

To demonstrate that coumarin and 5-fluorouracil retain their anticancer activity after conjugation with PEG, a preliminary *in vitro* cytotoxicity MTT assay was carried out. The cytotoxicity of blank micelles against PANC-1 and BxPC-3 cells was evaluated at two incubation times (24 h and 40 h). As shown in Figure 4, **CouPEG** and **5-FUPEG** exhibited a significant cytotoxicity in both human cancer pancreatic cells at the tested concentrations (25.6 and 51 µg/mL for **CouPEG**; 14.5, 22.4, 29, and 44.8 µg/mL for **5-FUPEG**).

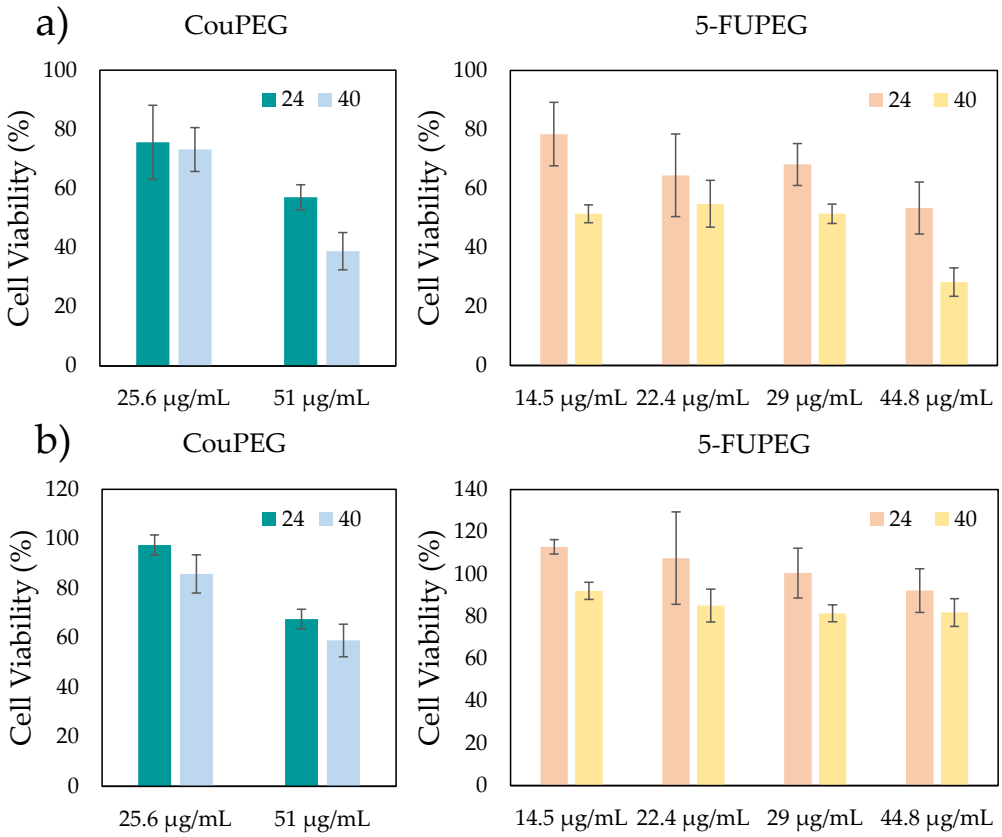

Figure 4. Cell viability of a) PANC-1 cells and b) BxPC-3 cells treated with **CouPEG** and **5-FUPEG** micelles at different doses after 24 and 40 h of incubation time.

Figure 4a shows the cell viability of **CouPEG** and **5-FUPEG** micelles in PANC-1 cells. PANC-1 cells gradually decreased their viability with the increase of conjugate concentration, which indicated a dose-dependent antiproliferative activity. A prolonged incubation time also promoted an increased cell death. Similar results were observed when BxPC-3 cells were treated with **CouPEG** micelles (Figure 4b, left). Regarding the **5-FUPEG** micelles, cell proliferation (hormetic effect) was observed at concentrations lower than 29 µg/mL and 24 h of incubation. Nevertheless, at higher concentrations, the cells gradually decreased their viability again (Figure 4b, right). Hormesis is widely found in a great variety of chemotherapeutic agents (included **5-FU**) and natural compounds isolated from plants [44-46]. These results indicated that the anticancer activity of curcumin and 5-fluorouracil is maintained in the **5-FUPEG** and **CouPEG** micelles, showing a significant cytotoxic effect on PANC-1 and BxPC3 cells.

4. Conclusions

Two novel amphiphilic coumarin- and 5-fluorouracil-PEG conjugates, **CouPEG** and **5-FuPEG**, have been prepared via a CuAAC reaction. It has been demonstrated that these polymer-drug conjugates self-assemble into regular micelles with an inner hydrophobic core. The large portion of hydrophilic PEG appears to be responsible for the relatively high critical micellar concentration determined by using the iodine UV-vis spectroscopy method. The potential of the micelles to load other anticancer agents such as paclitaxel, curcumin, and gemcitabine were studied for co-delivery and synergistic combination therapy. Drug loading capacity, encapsulation efficiency, particle size, and zeta potential studies showed that

paclitaxel and curcumin were efficiently loaded, obtaining sustained and controlled *in vitro* drug release profiles. In contrast, the low stability observed for the gemcitabine-loaded micelles led to an uncontrolled burst release of drug. The micelles also exhibited a dose-dependent antiproliferative activity against human pancreatic cancer cell lines PANC-1 and BxPC-3. These results provide a novel strategy for the development of promising co-delivery carriers for synergistic cancer therapy.

CRediT authorship contribution statement

Sonia López: conceptualization, investigation, writing–original draft preparation, writing–review and editing. **M. Jesús Ramos:** conceptualization, validation, supervision, project administration, funding acquisition. **M. Teresa García:** validation, project administration, funding acquisition. **Juan F. Rodríguez:** validation, project administration, funding acquisition. **José M. Pérez-Ortiz:** investigation, validation, writing–original draft preparation, supervision. **Julián Rodríguez-López:** investigation, validation, writing–original draft preparation, writing–review and editing. Supervision. **Ignacio Gracia:** conceptualization, validation, supervision, project administration, funding acquisition.

Declaration of competing interest

The authors declare no conflict of interest.

Acknowledgement

This research was funded by the Ministerio de Economía y Competitividad/Agencia Estatal de Investigación/FEDER is gratefully thanked (Project PID2019-109923GB-I00). S. L. gratefully acknowledges a FPI doctoral fellowship (Ref. BES-2017-079770).

Appendix A. Supplementary data

Supplementary data to this article can be found online at https://doi.org/10.1016/j.jddst.2022....

References

[1] World Health Organization (WHO), Latest global cancer data: cancer burden rises to 18.1 million new cases and 9.6 million deaths in 2018, International Agency for Research on Cancer (IARC), Geneva, 2018. Press release available from: https://www.iarc.fr/wp-content/uploads/2018/09/pr263_E.pdf (accessed May 28, 2022).

[2] F. Bray, M. Laversanne, E. Weiderpass, I. Soerjomataram, The ever-increasing importance of cancer as a leading cause of premature death worldwide, Cancer 127 (2021) 3021–3030. https://doi.org/10.1002/cncr.33587.

[3] H. Sung, J. Ferlay, R. L. Siegel, M. Laversanne, I. Soerjomataram, A. Jemal, F. Bray, Global cancer statistics 2020: GLOBOCAN estimates of incidence and mortality worldwide for 36 cancers in 185 countries, CA: Cancer J. Clin. 71 (2021) 209–249.

[4] C. Pucci, C. Martinelli, G. Ciofani, Innovative approaches for cancer treatment: current perspectives and new challenges, Ecancermedicalscience 13 (2019) 961. https://doi.org/10.3332/ecancer.2019.961.

[5] D.J. Irvine, E.L. Dane, Enhancing cancer immunotherapy with nanomedicine, Nat. Rev. Immunol. 20 (2020) 321–334. https://doi.org/10.1038/s41577-019-0269-6.

[6] N. Avramović, B. Mandić, A. Savić-Radojević, T. Simić, Polymeric nanocarriers of drug delivery systems in cancer therapy, Pharmaceutics 12 (2020) 298. https://doi.org/10.3390/pharmaceutics12040298.

[7] Z.G. Chen, Small-molecule delivery by nanoparticles for anticancer therapy, Trends Mol. Med. 16 (2010) 594–602. https://doi.org/10.1016/j.molmed.2010.08.001.

[8] B. Ghosh, S. Biswas, Polymeric micelles in cancer therapy: state of the art, J. Control. Release 332 (2021) 127–147. https://doi.org/10.1016/j.jconrel.2021.02.016.

[9] Q. Pan, X. Deng, W. Gao, J. Chang, Y. Pu, B. He, Small molecules-PEG amphiphilic conjugates as carriers for drug delivery: 1. the effect of molecular structures on drug encapsulation, J. Drug Deliv. Sci. Technol. 60 (2020) 101997. https://doi.org/10.1016/j.jddst.2020.101997.

[10] Q. Feng, R. Tong, Anticancer nanoparticulate polymer-drug conjugate, Bioeng. Transl. Med. 1 (2016) 277–296. https://doi.org/10.1002/btm2.10033.

[11] G. Pasut, F.M. Veronese, Polymer–drug conjugation, recent achievements and general strategies, Prog. Polym. Sci. 32 (2007) 933–961. https://doi.org/10.1016/ j.progpolymsci.2007.05.008.

[12] K. Shiraishi, M. Yokoyama, Toxicity and immunogenicity concerns related to PEGylated-micelle carrier systems: a review, Sci. Technol. Adv. Mater. 20 (2019) 324–336. https://doi.org/10.1080/14686996.2019.1590126.

[13] M. Al-Amili, Z. Jin, Z. Wang, S. Guo, Self-assembled micelles of amphiphilic PEGylated drugs for cancer treatment, Curr. Drug Targets 22 (2021) 870–881. https://doi.org/10.2174/1389450122666201231130702.

[14] R. Pola, A. Braunová, R. Laga, M. Pechar, K. Ulbrich, Click chemistry as a powerful and chemoselective tool for the attachment of targeting ligands to polymer drug carriers, Polym. Chem. 5 (2014) 1340–1350. https://doi.org/10.1039/c3py01376f.

[15] S. Neumann, M. Biewend, S. Rana, W.H Binder, The CuAAC: principles, homogeneous and heterogeneous catalysts, and novel developments and applications. Macromol. Rapid Commun. 41 (2020) 1900359. https://doi.org/10.1002/ marc.201900359.

[16] N. Nebra, J. García-Álvarez, Recent progress of Cu-catalyzed azide-alkyne cycloaddition reactions (CuAAC) in sustainable solvents: glycerol, deep eutectic solvents, and aqueous media, Molecules 25 (2020) 2015. https://doi.org/ 10.3390/molecules25092015.

[17] J. Hou, X. Liu, J. Shen, G. Zhao, P.G. Wang, The impact of click chemistry in medicinal chemistry, Expert Opin. Drug Discov. 7 (2012) 489–501. https://doi.org/10.1517/ 17460441.2012.682725.

[18] K. Slanova, L. Todorov, N.P. Belskaya, M.A. Palafox, I.P. Kostova, Developments in the application of 1,2,3-triazoles in cancer treatment, Recent Pat. Anticancer Drug Discov. 15 (2020) 92–112. https://doi.org/10.2174/1574892815666200717164457.

[19] V. Ciaffaglione, M.N. Modica, V. Pittalà, G. Romeo, L. Salerno, S. Intagliata, Mutual prodrugs of 5-fluorouracil: from a classic chemotherapeutic agent to novel potential anticancer drugs, ChemMedChem 16 (2021) 3496–3512. https://doi.org/10.1002/ cmdc.202100473.

[20] A. Thakur, R. Singla, V. Jaitak, Coumarins as anticancer agents: a review on synthetic strategies, mechanism of action and SAR studies, Eur. J. Med. Chem. 101 (2015) 475–495. https://doi.org/10.1016/j.ejmech.2015.07.010.

[21] J. Gallego-Jara, G. Lozano-Terol, R.A. Sola-Martínez, M. Cánovas-Díaz, T. de Diego Puente, A compressive review about Taxol®: history and future challenges, Molecules 25 (2020) 5986. https://doi.org/10.3390/molecules25245986.

[22] S.J. Hewlings, D.S. Kalman, Curcumin: a review of its effects on human health, Foods 6 (2017) 92. https://doi.org/10.3390/foods6100092.

[23] M.A. Tomeh, R. Hadianamrei, X. Zhao, A review of curcumin and its derivatives as anticancer agents, Int. J. Mol. Sci. 20 (2019) 1033. https://doi.org/10.3390/ ijms20051033.

[24] E. Moysan, G. Bastiat, J.-P. Benoit, Gemcitabine versus modified gemcitabine: a review of several promising chemical modifications, Mol. Pharmaceutics 10 (2013) 430–444. https://doi.org/10.1021/mp300370t.

[25] P.A. Gerken, J.R. Wolstenhulme, A. Tumber, S.B. Hatch, Y. Zhang, S. Müller, S.A. Chandler, B. Mair, F. Li, S.M.B. Nijman, R. Konietzny, T. Szommer, C. Yapp, O. Fedorov, J.L.P. Benesch, M. Vedadi, B.M. Kessler, A. Kawamura, P.E. Brennan, M.D. Smith, Discovery of a highly selective cell-active inhibitor of the histone lysine demethylases KDM2/7, Angew. Chem. Int. Ed. 56 (2017) 15555–15559. https://doi.org/10.1002/anie.201706788.

[26] S.A. Caldarelli, S. El Fangour, S. Wein, C. Tran van Ba, C. Périgaud, A. Pellet, H.J. Vial, S. Peyrottes, New bis-thiazolium analogues as potential antimalarial agents: design, synthesis, and biological evaluation, J. Med. Chem. 56 (2013) 496–509. https://doi.org/10.1021/jm3014585.

[27] S. López, I. Gracia, M.T. García, J.F. Rodríguez, M.J. Ramos, Synthesis and operating optimization of the PEG conjugate via CuAAC in $scCO_2$, ACS Omega 6 (2021) 6163–6171. https://doi.org/10.1021/acsomega.0c05466.

[28] J.T. Mehl, R. Murgasova, X. Dong, D.M. Hercules, H. Nefzger, Characterization of polyether and polyester polyurethane soft blocks using MALDI mass spectrometry, Anal. Chem. 72 (2000) 2490–2498. https://doi.org/10.1021/ac991283k.

[29] I. Kaur, K.M. Kosak, M. Terrazas, J.N. Herron, S.E. Kern, K.M. Boucher, P.J. Shami, Effect of a Pluronic® P123 formulation on the nitric oxide-generating drug JS-K, Pharm. Res. 32 (2015) 1395–1406. https://doi.org/10.1007/s11095-014-1542-9.

[30] R.W. Korsmeyer, R. Gurni, E. Doelker, P. Buri, N.A. Peppas, Mechanisms of solute release from porous hydrophilic polymers, Int. J. Pharm. 15 (1983) 25–35. https://doi.org/10.1016/0378-5173(83)90064-9.

[31] P.L. Ritger, N.A. Peppas, A simple equation for description of solute release I. Fickian and non-fickian release from non-swellable devices in the form of slabs, spheres, cylinders or discs, J. Control. Release 5 (1987) 23–36. https://doi.org/10.1016/0168-3659(87)90034-4.

[32] P.L. Ritger and N.A. Peppas, A simple equation for description of solute release II. Fickian and anomalous release from swellable devices, J. Control. Release 5 (1987) 37–42. https://doi.org/10.1016/0168-3659(87)90035-6.

[33] *Molinspiration Chemoinformatics software*. https://www.molinspiration.com/cgi-bin/properties (accessed February 14, 2022).

[34] G. Behl, M. Sikka, A. Chhikara, M. Chopra, PEG-coumarin based biocompatible self-assembled fluorescent nanoaggregates synthesized via click reactions and studies of aggregation behavior, J. Colloid Interface Sci. 416 (2014) 151–160. https://doi.org/10.1016/j.jcis.2013.10.057.

[35] H. Yu, Q. Huang, Enhanced in vitro anti-cancer activity of curcumin encapsulated in hydrophobically modified starch, Food Chem. 119 (2010) 669–674. https://doi.org/10.1016/j.foodchem.2009.07.018.

[36] J. Liu, H. Lee, C. Allen, Formulation of drugs in block copolymer micelles: drug loading and release, Curr. Pharm. Des. 12 (2006) 4685–4701. https://doi.org/10.2174/138161206779026263.

[37] A. Kapse, N. Anup, V. Patel, G.K. Saraogi, D.K. Mishra, R.K. Tekade, Polymeric micelles: a ray of hope among new drug delivery systems, in: R.K. Tekade (Ed.), Drug Delivery Systems, Academic Press, 2020, Chap. 6, pp. 235–289. https://doi.org/10.1016/B978-0-12-814487-9.00006-5.

[38] M. Yokoyama, P. Opanasopit, T. Okano, K. Kawano, Y. Maitani, Polymer design and incorporation methods for polymeric micelle carrier system containing water-insoluble anti-cancer agent camptothecin, J. Drug Target. 12 (2004) 373–384. https://doi.org/10.1080/10611860412331285251.

[39] V.B. Patravale, P.G. Upadhaya, R.D. Jain, Preparation and characterization of micelles, in: V. Weissig, T. Elbayoumi, (Eds.), Pharmaceutical Nanotechnology: Basic Protocols, Humana Press, New York, 2019, Chap. 2, pp. 19–29. https://doi.org/10.1007/978-1-4939-9516-5_2.

[40] A. Mahmud, X.-B. Xiong, A. Lavasanifar, Novel self-associating poly(ethylene oxide)-block-poly(ε-caprolactone) block copolymers with functional side groups on the polyester block for drug delivery, Macromolecules 39 (2006) 9419–9428. https://doi.org/10.1021/ma0613786.

[41] M. Danaei, M. Dehghankhold, S. Ataei, F.H. Hasanzadeh Davarani, R. Javanmard, A. Dokhani, S. Khorasani, M.R. Mozafari, Impact of particle size and polydispersity index on the clinical applications of lipidic nanocarrier systems, Pharmaceutics 10 (2018) 57. https://doi.org/10.3390/pharmaceutics10020057.

[42] J. Yoo, Y.-Y. Won, Phenomenology of the initial burst release of drugs from PLGA microparticles, ACS Biomater. Sci. Eng. 6 (2020) 6053–6062. https://doi.org/10.1021/acsbiomaterials.0c01228.

[43] J. Chang, Y. Li, G. Wang, B. He, Z. Gu, Fabrication of novel coumarin derivative functionalized polypseudorotaxane micelles for drug delivery, Nanoscale 5 (2013) 813–820. https://doi.org/10.1039/c2nr32927a.

[44] E.J. Calabrese, Cancer biology and hormesis: human tumor cell lines commonly display hormetic (biphasic) dose responses, Crit. Rev. Toxicol. 35 (2005) 463–582. https://doi.org/10.1080/10408440591034502.

[45] E.J. Calabrese, Hormetic mechanisms, Crit. Rev. Toxicol. 43 (2013) 580–606. https://doi.org/10.3109/10408444.2013.808172.

[46] M.C. Alley, C.M. Paculacox, M.L. Hursey, L.R. Rubinstein, M.R. Boyd, Morphometric and colorimetric analyses of human tumor-cell line growth and drug sensitivity in soft agar culture, Cancer Res. 51 (1991) 1247–1256.